Validation of deformable dose accumulation for image guided radiotherapy using a deformable dosimeter insert

Laurie J.M. de Vries
Department of Radiotherapy
University Medical Center Utrecht
Utrecht, The Netherlands
l.j.m.devries-30@umcutrecht.nl

Supervisors:
Madelon van den Dobbelsteen, Lando S. Bosma
Cornel Zachiu, Sara L. Hackett
Department of Radiotherapy, UMC Utrecht

Abstract

Background and purpose: Image-guided radiotherapy (IGRT) enables visualization of the anatomy and anatomical changes. Due to changes, the dose can end up in a different location than initially planned. Taking changes into account for dose accumulation is done with deformable image registration (DIR). The registration is done on the basis of images acquired during treatment. The validation of the accumulated dose remains challenging due to the lack of a ground truth. The purpose of this study is to investigate deformable dose accumulation and the usage of a novel deformable dosimeter as its validation.
Materials and methods: This study uses a prototype deformable insert containing six plastic scintillation dosimeters (PSDs) capable of measuring the dose real-time and allowing non-rigid deformations. Two experiments on the MR-linac were performed, a single-beam dose delivery and a multi-beam dose delivery. During both experiments non-rigid displacements took place and MR images were made. Three different DIR methods, optical flow, Elastix, and EVolution, and two warping methods, pulling and pushing, were utilized to obtain the accumulated dose.
Results: For the single-beam experiment the largest differences between planned and measured dose were 89% and -39% for the two PSDs mostly affected by motion. Dose differences between accumulated and measured were reduced to a maximum of 0.4% for all methods and all PSDs. For the multi-beam experiment the largest differences between planned and measured dose were 63% and -48% for the two PSDs mostly affected by motion. Dose differences between accumulated and measured were reduced to a maximum of 14% for all methods and all PSDs.
Conclusion: The novel prototype insert demonstrated its feasibility for validating deformable dose accumulation. Furthermore, all methods used in this study to obtain the accumulated dose were far superior to assuming the planned dose was delivered.

Keywords

deformable image registration, dose accumulation, IGRT, MR-linac, quality assurance

I. Introduction

External beam radiotherapy is a medical treatment that uses radiation to non-invasively target and destroy cancer cells. During treatment, the goal is to deliver a high dose to the tumor while minimizing exposure to surrounding tissue and the organs at risk (OARs). Achieving precise dose delivery is challenging due to physiological and anatomical changes, caused by, for example, respiration. The positional uncertainties, due to factors such as motion, necessitate the addition of margins to the target area, to avoid underdosage to the tumor. This results in a larger volume of healthy tissue receiving unnecessary dose.

To deliver the dose more accurately, an imaging device can be used before and during the course of treatment. Image-guided radiotherapy (IGRT) facilitates visualization of anatomical structures within the treatment field [1]. At the UMC Utrecht, an MR-linac system is available for the delivery of IGRT treatments. The MR-linac is a combination of a linear accelerator for irradiation with a magnetic resonance imaging (MRI) system providing real-time soft-tissue visualization [2], [3]. Using the excellent soft-tissue contrast of MRI without additional irradiation for imaging, the MR-linac offers unparalleled treatment guidance and monitoring capabilities. In the current IGRT workflow, radiation plans are updated based on the patient's anatomy on the day of treatment. This approach allows for the correction of interfractional motion, i.e. motion that occurs in between fractions. This accounts for changes due to digestive and physiological activity, such as changes in bladder filling or positioning [4]. Consequently, the large treatment fields, necessitated by positional uncertainties, can be reduced due to increased positional accuracy afforded by IGRT [5]. In addition, anatomical changes also occur during the treatment session, such as respiratory motion, this is called intrafractional motion [6]. This could be managed by dynamic intrafractional adjustments to the treatment plan and this accounts for anatomical changes during the fraction [7]. The pursuit of adaptive treatment strategies emphasizes the overarching goal of tumor motion tracking. By dynamically adjusting radiation delivery to account for real-time tumor movement, the aim is to maximize treatment efficacy while minimizing the risk of off-target irradiation.

By integrating imaging modalities directly into the treatment workflow, IGRT enables reconstruction of the delivered dose. This can be done both interfractional and intrafractional. The changes between the configurations can be estimated using deformable image registration (DIR). DIR methods facilitate the transformation of the voxels in the image. This displacement information provides us with a deformation vector field (DVF). Due to anatomical changes that occur during treatment, the dose maps cannot be directly summed, because the position of the irradiated tissue could have changed. All partial delivered doses can be mapped to a common reference position. Summing up all these partial delivered mapped doses gives the accumulated dose that takes the anatomical changes into account. The process of dose accumulation can reveal discrepancies between the planned dose and the delivered dose. The next step could be to adapt and optimize the subsequent radiation delivery by using the reconstructed delivered doses. This can be done inter- and intra-fractionally. Although dose accumulation is not yet clinically implemented, partly due to the lack of its validation, it is anticipated to become essential for adaptive radiotherapy to offer a comprehensive view of the total delivered dose [8], [9]. Therefore, the validation of deformable dose accumulation in IGRT is of great importance.

One of the primary challenges in dose accumulation is the absence of a definitive ground truth, making it difficult to determine the most effective and accurate method for obtaining the reconstructed dose. However, various approaches can be employed to evaluate the performance of deformable dose accumulation. One approach to establish a ground truth is by measuring the delivered dose. However, obtaining accurate dose measurements with dosimeters in the presence of a magnetic field and MRI gradients can be challenging. The presence of a magnetic field induces the Lorentz force, which affects the trajectory of secondary electrons, potentially leading to incorrect dose estimations. Nevertheless, it is possible to account for these effects to ensure accurate measurements [10]. Film dosimetry, which is usable within a magnetic field, has been identified as a useful method for validating dose delivery. This dosimetry method has been applied in several studies on dose accumulation. For example, in a phantom that represents the specific

anatomical regions such as the rectum [11], in a deformable pelvis phantom [12], and for an end-to-end validation of dose delivery on the MR-linac [13].

However, for the experiments done in this study, we will not utilize film dosimetry, since it is unable to measure the dose in real-time and it is impractical for non-rigid deformations from one measurement point relative to another. Instead, plastic scintillator dosimeters (PSDs) will be used to measure the dose and provide us with a validation for our deformable accumulated dose. PSDs are suitable for this study, since they are able to measure the dose real-time in a point and the different measurement points can move non-rigidly relative to each other. The PSDs convert the incoming radiation dose into a proportional amount of optical photons through scintillation. The photon flux is measured by a read-out system, which converts the photons into a normalized dose value. The PSDs used in this study are compatible with 1.5 T MR systems [14]. Additionally, the PSDs do not interfere with the MR signal that was acquired. Due to their ability to move non-rigidly relative to each other, their compatibility with MR-linac environments and their ability to measure the dose real-time, PSDs are well suited to be used in this study.

By providing experimental validation of this deformable dose accumulation, further precision in IGRT workflows can be developed. This paper investigates the potential of a prototype deformable insert that can measure the dose in real-time, facilitating the validation of deformable dose accumulation within the context of IGRT. In the experiments performed, we utilized various DIR methods to achieve this and evaluate the accuracy of the estimated dose using the prototype insert.

II. Materials & Methods

In this section, we describe the prototype deformable insert, explain the experiments performed and give an overview of the methods used in the process of deformable dose accumulation. Additionally, we outline the methods used to analyze and validate the results.

A. Deformable Insert Prototype

For the experiments performed, a prototype deformable insert [15] was used (Fig. 1). The insert can be connected to a motor via the piston at the top, enabling movement (Fig. 2). The diameter of the insert is approximately 8 cm. When the piston is fully inserted, the cylindrical insert has a total length of 25 cm. The insert contains an egg-shaped structure, which will be considered as the gross target volume (GTV) for the scope of this work. The GTV is surrounded by foam, with a relative electron density of 1.0, thus water-equivalent. The GTV is visible and distinguishable from its surroundings on MR images. The deformable insert can be controlled by the piston to allow non-rigid deformation within the GTV, causing the longer axis of the egg-shaped GTV to vary between 3 and 4 cm.

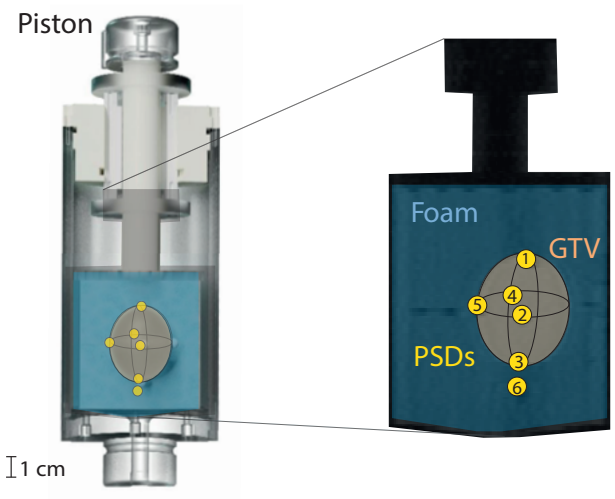

Fig. 1. The deformable insert prototype showing the gross target volume (GTV), foam and indicating the places of the plastic dosimeter scintillators (PSDs) (adapted from [16]).

The insert contains six HYPERSCINT plastic scintillation dosimeters (PSDs) (Medscint, Quebec City, QC), which are MR-compatible and are able to obtain the dose in real-time [14] . Five out of six PSDs are located inside the GTV, the other one is positioned just outside the GTV. The placements of the PSDs are visualized in Fig. 1, with PSD 2 in the center of the GTV and PSD 1, PSD 3, PSD 4, and PSD 5 on the surface of the egg-shaped GTV. The exact positions of the PSDs are controlled by the piston position.

Two different insert prototypes were used in this study. The primary difference lies in the way the fibers from the PSDs exited the insert. In the first prototype, the fibers from the PSDs had a short exit path. The fibers in the second prototype featured a spiral configuration around the GTV. Another minor difference is the relative electron density of the GTV, this is equal to 1.091 and 1.094 for the two prototypes respectively. The exact locations of the PSDs also varied between the two prototypes, hence, they were not used interchangeably. The number of scintillators within and outside the GTV remained consistent.

B. Experiments

During the experiments, the deformable insert is placed in QUASAR MRI^{4D} motion phantom (IBA QUASAR, London, ON) (Fig. 2). The phantom consisted of an oval body filled with water, with dimensions of 20 cm in length, 30 cm in width and 20 cm in height. The insert was connected to a motor via the piston capable of inducing the non-rigid deformations. The piston moved in the superior-inferior direction, indicated with a yellow arrow (Fig. 2), with a range of motion between -17.5 mm up to 17.5 mm and a motion precision of ± 0.25 mm[1].

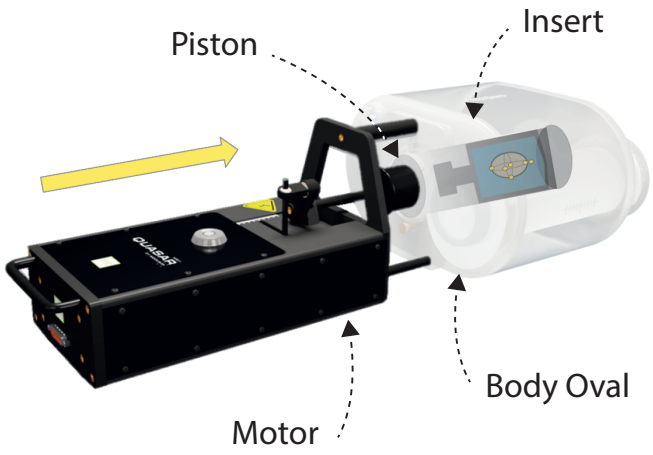

Fig. 2. The deformable insert prototype inside of the QUASAR MRI^{4D} motion phantom, with the yellow arrow providing the direction of the piston movement, superior-inferior (adapted from [16]).

[1]www.iba-dosimetry.com/product/quasar-mri4d-motion-phantom

All measurements were performed at the 1.5 T Unity MR-linac (Elekta AB, Stockholm, Sweden). For all experiments, the piston position was adjusted ranging from piston position 0 mm to -17.5 mm taking seven steps of 2.5 mm each. At each of the eight positions, a 3D MR scan with a voxel size of $0.64 \times 0.64 \times 1.0$ mm^3 was acquired and used as the input for the DIR methods, as will be described in section C.

Two experiments were performed, one on each prototype, using different treatment plans. For experiment A, the dose was calculated using Monaco v5.51.10 (Elekta AB, Stockholm, Sweden) by making use of the relative electron density of the GTV obtained from a CT scan acquired at piston position 0 mm. The rest of the densities are overwritten to 1, as they were assumed water-equivalent. The measurements were performed for a static beam with a size of 3.7×4.2 cm^2, delivering 400 MU from a gantry angle of 0°. For the second experiment, experiment B, the dose was also calculated using Monaco, by making use of the electron density information from a CT scan at piston position 0 mm for the GTV. For these measurements, four static beams with a size of 4×4.5 cm^2, shaped as a box around the GTV, delivered 200 MU from gantry angles 0°, 90°, 180°, and 270°. These four beams were delivered for all eight piston positions, delivering 800 MU in total. For both dose plans, the higher dose region is located around the GTV, aiming to deliver a high dose to PSD 1 - PSD 5 (within the GTV) and a low dose to PSD 6 (outside the GTV).

C. Deformable Dose Accumulation

During both experiment A and B, MR images were acquired on the MR-linac. These images capture the deformable insert in each of the eight piston positions. In both experiments, the reference position is at piston position 0 mm, this is also the position at which the CT scan is made and where the planned dose is based on. All the DIR methods thus estimated the displacement field that describes how each point in the reference image, the MR at piston position 0, moves to its corresponding point in the moving image, the MR at piston position ranging from 0 mm to -17.5 mm. All DIR for this study is done on MR-images.

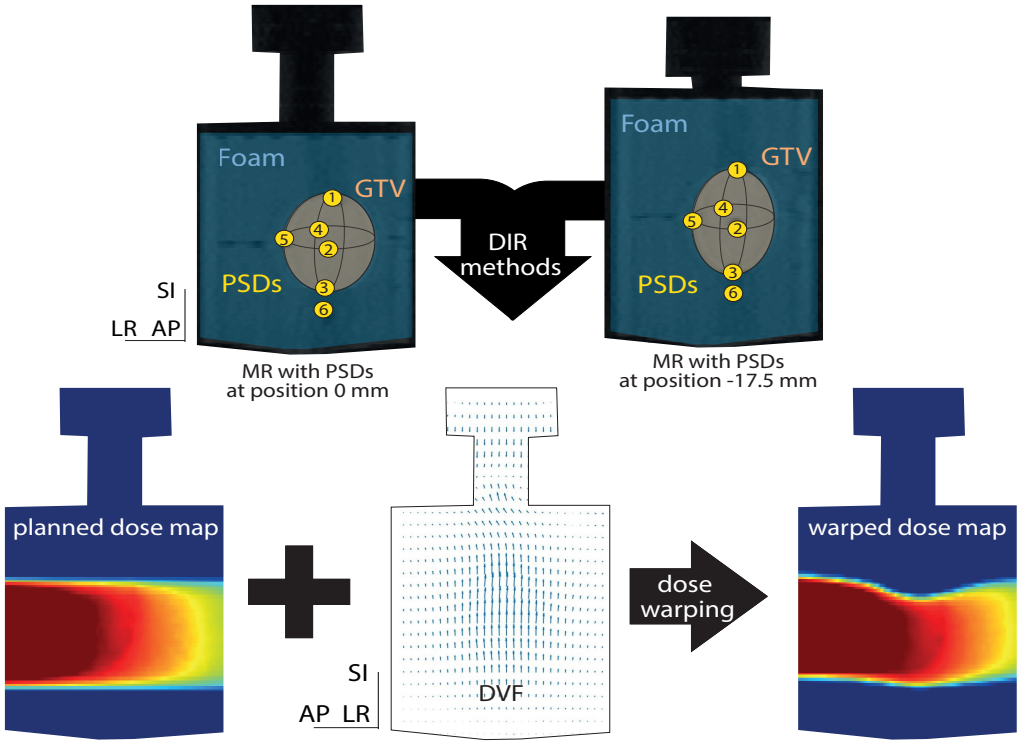

Fig. 3. A schematic overview of how the warped dose is obtained. First, deformable image registration (DIR) is applied to the top two MR images, resulting in the deformation vector fields (DVFs). Second, the DVFs are used for dose warping, resulting in the warped dose map.

Three different DIR methods were used in both experiments: optical flow [17], Elastix [18] and EVolution [19]. Optical flow and Elastix are both intensity-based image registration methods, EVolution is a contrast-based method. The optical flow algorithm assumes that the image intensities are conserved, but are able to change in position. The Elastix algorithm optimizes mutual information by making use of B-spline regularization. The EVolution algorithm aims to align the intensity boundaries by looking at the image gradients. All three are used in the field of medical imaging. For experiment A, the previously established parameters of the DIR methods were briefly reviewed and reused in experiment B.

To sum the doses, all partial doses were mapped to the reference position, by applying the DVFs obtained by DIR methods. This mapping is called dose warping and for this study two different strategies were used. For pulling (backward warping), for each voxel in the warped dose map, the algorithm determines where it came from in the input image (planned dose). For pushing (forward warping), for each voxel in the input image (planned dose) the algorithm determines its new position in the warped image [20], [21]. Pulling (backward warping) uses the inverse DVFs from pushing (forward warping). The entire process of arriving at an approximation of the total delivered dose at a reference position, is known as deformable dose accumulation (Fig. 3).

D. Validation

For both experiments, a visual comparison was done for validating the different DIR and warping methods that were used. To evaluate the accuracy of the accumulated deformable dose, it would be ideal to compare it with the actual delivered dose. The PSDs (plastic scintillation detectors) inside the deformable insert were used to measure the dose in real-time, providing an estimation of the delivered dose in

the six points where the PSDs were placed. The planned dose was calculated using Monaco, and the accumulated doses were derived using different DIR methods. These doses were compared by taking the absolute differences with the measured dose. The dose differences between the planned and measured doses were compared to the dose differences between the accumulated and measured doses.

The voxel location of the sensitive volume of the PSDs was determined from the MR scan visually. The sensitive volumes were positioned in an envelope, which can be properly identified on MR-scans. Due to uncertainty in the exact location of the sensitive volume within this envelope, the measured doses were compared to the planned and accumulated doses within a neighborhood. For experiment A, the neighborhood includes ten surrounding voxels, one in each direction, providing a ± 1 mm range of positional uncertainty. For experiment B, a smaller positional uncertainty of ± 0.5 mm was taken into account. This was done by taking eight neighborhood voxels within the same slice as the visually selected sensitive volume and the average of the visually selected voxel and a voxel in the perpendicular direction, superior as well as inferior, into account for the positional uncertainty. The absolute dose differences were determined using the closest dose value within this positional uncertainty.

For the prototype used in experiment B, a reduction of sensitivity for the PSDs was observed. The response of the PSDs to a specific dose reduced over time. To account for this reduction, an error bar was added to the measured doses. The doses were measured one hour after the initial measurements, and by assuming that the reduction was linear, an estimation of the reduction was made. This reduction of sensitivity was determined individually for each PSD.

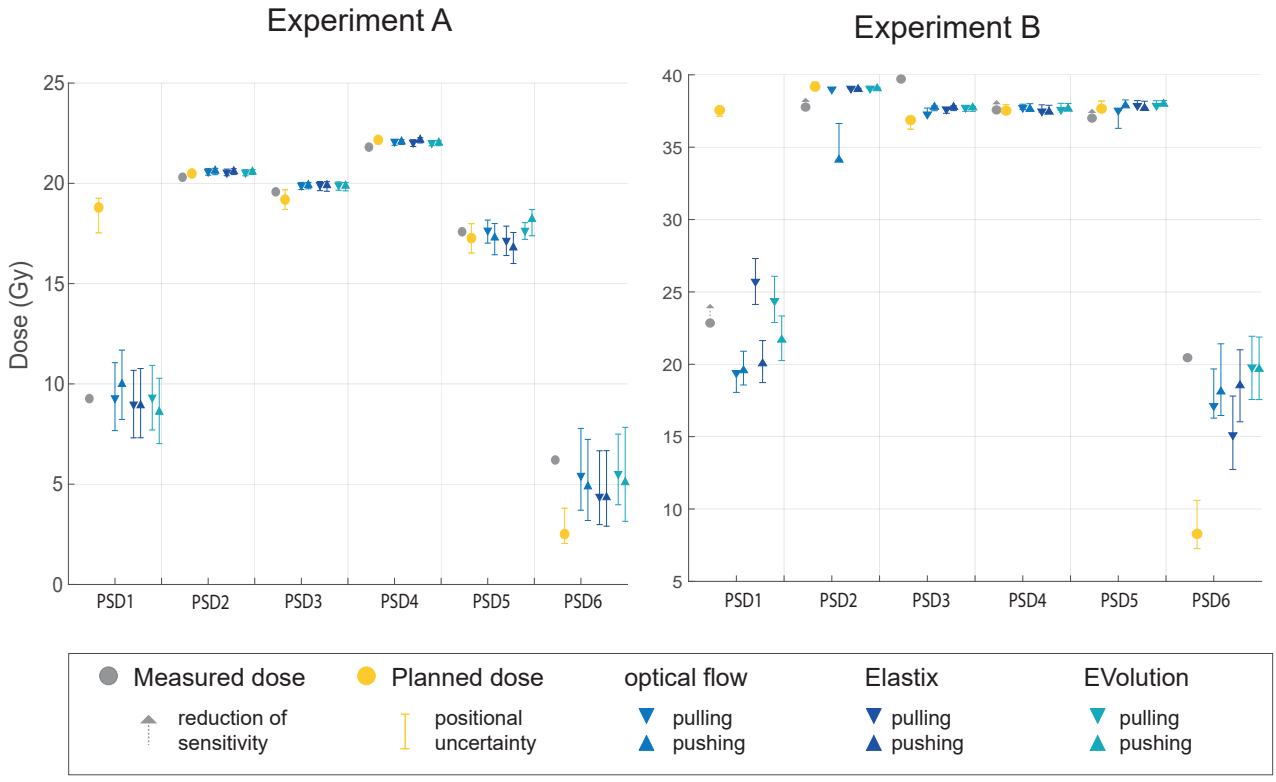

Fig. 4. For experiment A (left side): The planned, measured and calculated accumulated doses, including error bars representing the positional uncertainty of the location of the PSDs sensitive volume. For experiment B (right side): The planned, measured and calculated accumulated doses, including error bars representing the positional uncertainty of the location of the PSDs sensitive volume and dotted lines on the measured dose representing the reduction of sensitivity for the PSDs.

III. Results

A. Accumulated doses

For experiment A, the resulting total doses for the different deformable dose accumulation methods, planned, and measured, including the positional uncertainty, are plotted on the left side of figure 4. For this experiment, the differences in dose between the planned and measured doses were observed to be 0.08 Gy, 0 Gy, 0.17 Gy and 0 Gy respectively for PSDs 2-5, taking the positional uncertainty into account. For those PSDs, this resulted in a maximum absolute dose difference of 0.8%. For PSD 1 a difference of 8.27 Gy was observed, resulting in a dose difference of 89% between planned and measured. For PSD 6 a difference of -2.4 Gy was observed, resulting in a dose difference of -39% between planned and measured.

For experiment A, the accumulated dose for all three DIR methods, optical flow, Elastix, Evolution, and two different warping techniques, pulling and pushing, showed aligned results and a better agreement with the measured dose compared to the planned dose. Maximum dose differences of 0.4% were observed for all PSDs and dose accumulation methods when positional uncertainty is taken into account.

For the second experiment, experiment B, the planned, measured, and accumulated doses, including positional uncertainty and an error bar for reduction of the sensitivity of the PSDs, are plotted on the right side of figure 4. For this experiment, the differences in dose between the planned and measured doses were observed to be 1.41 Gy, -2.73 Gy, 0 Gy and 0.66 Gy respectively for PSDs 2-5, taking the positional uncertainty into account. For those PSDs, this resulted in a maximum absolute dose difference of 6.8%. For PSD 1 a difference of 14.3 Gy was observed, resulting in a dose difference of 63% between planned and measured. For PSD 6 a difference of -9.86 Gy was observed, resulting in a dose difference of -48% between planned and measured.

For experiment B, the accumulated dose for all three DIR methods, optical flow, Elastix, Evolution, and two different warping techniques, pulling and pushing, show aligned results and a better agreement with the measured dose compared to the planned dose.

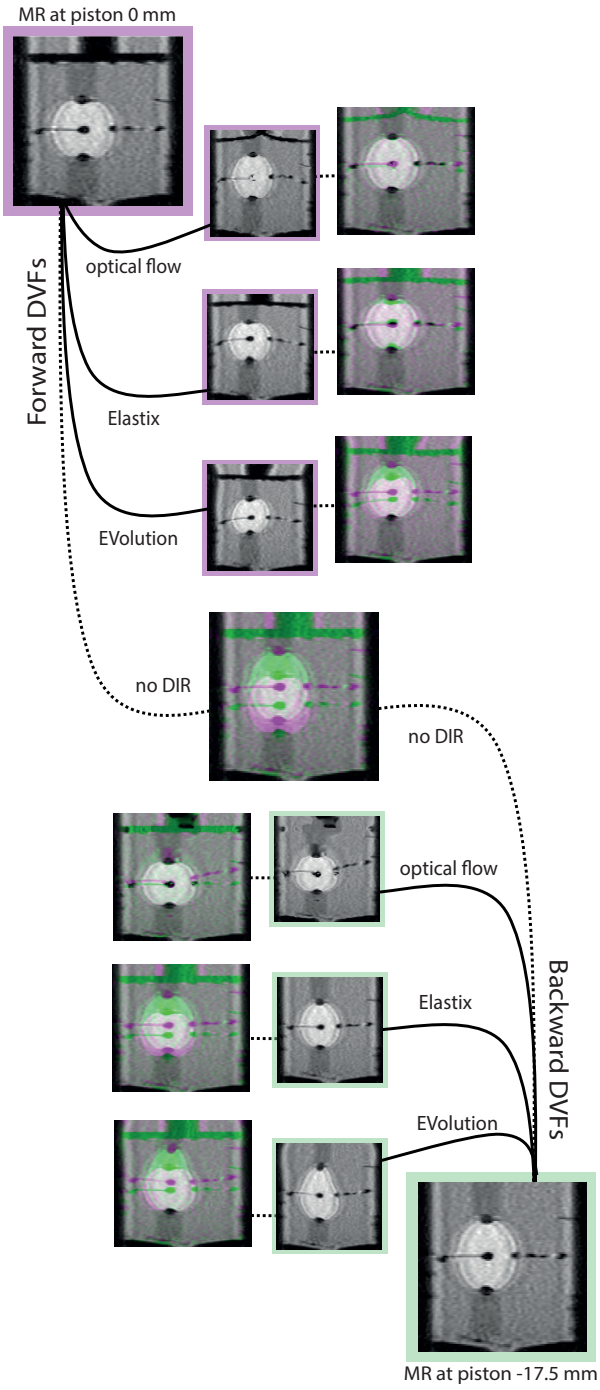

Fig. 5. Visualization of the forward and backward deformable vector fields (DVFs) applied on MR images to see the performance of no registration and the performance of the three deformable image registration methods. The DVFs and MR images are both from experiment B.

Maximum dose differences of 14% were observed for all PSDs and dose accumulation methods when positional uncertainty is taken into account. For EVolution the maximum absolute dose difference was observed to be 4.8% for all PSDs.

B. Visualization of the DIR methods

The visualization of the different DIR methods for experiment A showed similar results for the different DIR methods used. For experiment B, a greater variation between the different DIR methods was observed. In figure 5, the results of DIR from piston position 0 to -17.5 mm for experiment B are shown. The image in the center illustrates the deformations occurring as the piston position is changed from 0 mm to -17.5 mm. The figure displays the forward DVFs applied to the MR scan at position 0 mm and the backward DVFs applied to the MR scan at position -17.5 mm. This analysis is done for DIR methods optical flow, Elastix and EVolution. Additionally, a noticeable dissimilarity between the forward and backward DVFs obtained with the same DIR method is visible for all three DIR methods. Note that in this figure, only the largest deformation of the experiment is shown.

IV. Discussion

The deformable insert demonstrated promising results for estimating the ground truth at the location of the six PSDs. Thereby it enables the validation of the performed deformable dose accumulation. Despite the fact that this is still a prototype and certain aspects require further optimization, the potential of this approach is evident. In this discussion some optimization and adjustment steps will be discussed. The use of real-time dosimeters, compatible with MR environments and able to move non-rigidly relative to each other, represents a significant step forward in the validation of deformable dose accumulation.

For experiment A, dose differences between planned and measured were observed to be 89% for PSD 1, an absolute maximum of 0.8% for PSDs 2-5, and -39% for PSD 6. The four PSDs 2-5 can be considered as a control group, since they remain in the high dose region. When applying any of the deformable dose accumulation methods, the differences compared to measured were reduced to a maximum of 0.4% for all PSDs within the positional uncertainty of 1 mm. For experiment B, dose differences between planned and measured were observed to be 63% for PSD 1, an absolute maximum of 6.9% for PSDs 2-5, and -48% for PSD 6. Again, PSDs 2-5 can be considered a control group. When applying any of the deformable dose accumulation methods, the differences compared to measured were reduced to a maximum of 14% for all PSDs within the positional uncertainty of 0.5 mm.

The improvements in agreement with the measured dose for both experiments suggest that the DIR methods, along with the warping techniques, provide a more accurate representation of the actual dose distribution. Thereby enhancing the reliability of dose accumulation. Therefore, this study provides an experimental validation of deformable dose accumulation via a deformable dosimeter insert. Indicating, regardless of the method used for obtaining the accumulated dose, there is a better agreement with the measured dose compared to the agreement between the planned and measured dose.

The current study used, as stated in the materials, two different insert prototypes. For the first prototype the fibers had a short exit path, causing too much bending due to deformation induced by the piston. Consequently, the second prototype featured a spiral configuration around the GTV, which resolved the bending-issue, but introduced new issues/challenges related to too small loops and too much fiber in the field caused by this spiral path. Regarding the reduction of sensitivity of the PSDs in experiment B, we observed that the PSDs with a longer path out of the insert, specifically PSD 1, followed by PSD 2, PSD 4, and PSD 5, experienced more significant reduction in the measured dose. This is likely due to irradiation through the fibers, which affects PSDs with a longer path out of the insert more severely. Another minor difference was the relative electron density of the GTV. This small density difference did not have an impact on the results. During the normalization of the PSDs in the deformable insert used in experiment B, PSD 3 and PSD 4 were swapped. Since both PSDs remained within the high-dose region, we estimated that this had a negligible impact on the measured dose.

For experiment A, the exact location of the sensitive volume inside the envelope could be slightly shifted. Whereas in experiment B, we have a higher certainty that the sensitive volume is positioned exactly in the center of the envelope. Therefore, the positional uncertainty of experiment A was ± 1 mm and for experiment B this was reduced to ± 0.5 mm. Knowledge of the exact location of the sensitive volume positions will reduce the geometric uncertainty, allowing for a more extensive validation.

For the experiments done in this study, the DIR methods are only applied to MR images. Applying DIR methods to input images that are both MR-images, provides an easier and more straightforward registration compared to registration between different image modalities. Handling different modalities is more challenging due to variations in image properties such as spatial resolution, contrast and noise characteristics. These properties are consistent within the MR images we used. The fact that the registration is more straightforward could be one of the reasons that it is difficult to determine the best performing dose accumulation method. Remarkable is the fact that for PSD 6, in both experiments and for all dose accumulation methods a lower accumulated dose was obtained compared to the measured dose. This is probably due to an underestimation of the motion of PSD 6. The lower obtained accumulated dose is clearly visible in figure 4. Especially for experiment B, DIR method Elastix and warping technique pulling. This corresponds with the underestimation of the motion. Which is visible in figure 5 for the backward DVFs obtained with Elastix, where PSD 6 is located just below the GTV.

For PSDs 2-5 in both experiments, the planned, measured, and accumulated doses were well aligned, as expected. However, for experiment B, the dose obtained in the position of PSD 2 with the DIR method optical flow and the warping technique pushing was unusually low. As known, pulling ensures complete coverage of the warped dose map, but does not necessarily use all the information available in the planned dose map. Pushing uses all the information from the planned dose map, but can result in gaps/empty voxels, in the warped dose map. This low dose can be explained by the fact that a gap was formed with the warping technique pushing that was used to obtain the accumulated dose (Fig. 6).

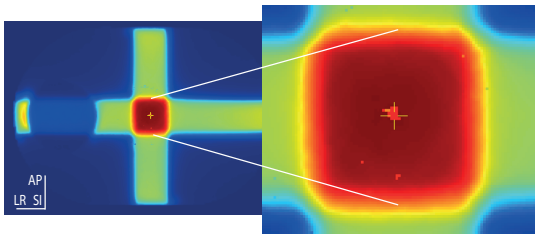

Fig. 6. The accumulated dose for experiment B, obtained with DIR method optical flow and warping method push. The yellow plus indicates the location of PSD 2. On the right side a zoomed in map around this scintillator is shown.

A. Comparison

Considerable research has been done on validating and obtaining the reconstructed dose. One study involved using a deformable phantom of the thoracic region [22]. However, this study lacked dosimeters, making it suitable only for visual image based validation. Other research has been conducted without a physical phantom, such as using a biomechanical patient model for the head and neck site to evaluate DIR methods [23] or motion compensated dose accumulation applied on simulations of radiation therapy for the prostate [24].

Research has also been conducted with physical phantoms capable of deformation while measuring the dose. Examples are the studies on a rectum phantom with film as a dosimeter [11] and one on a pelvis phantom using film strips as a dosimeter [12] and another example on a deformable gel phantom that was used to evaluate the performance of twelve different DIR methods [25]. Compared to our study, these lack the component of real-time dose measurement. Although this capability was not extensively utilized in our study, it is expected to play a more significant role in future evaluations, in for example the validation of deformable dose accumulation for tumor tracking treatments.

The lack of validation is currently limiting the clinical application of deformable dose accumulation [26]. Some components of our pipeline are not feasible for clinical application. For instance, in this study, the MR images were taken with a high resolution having a voxel size of $0.64 \times 0.64 \times 1.0$ mm^3 and large

dimensions of $704 \times 704 \times 220$. Acquiring these MR-images is time-consuming and, therefore, not practical when patients are in the scanner. Additionally, the performance of DIR differs for the insert compared to clinical scenarios. For the deformable insert, the deformations are small and it contains simpler and fewer structures, simplifying the registration process compared to clinical settings. On the other hand, the shearing within the insert results in less smooth DVFs, complicating the registration compared to clinical settings. Despite these discrepancies with the clinical scenarios, this study is the first to measure dose real-time on a deformable phantom, marking a significant step forward in the validation of deformable dose accumulation using a physical phantom.

B. Outlook

In future studies, the real-time component of the PSDs could be utilized. This offers more insight into the real-time dose behavior when dynamic motion is introduced to the piston instead of maintaining eight static positions. For the more dynamic motion, the high resolution MR images used in this study are not feasible. To capture the changes, Cine MRs can be employed. Applying DIR to obtain deformable dose accumulation to these Cine MRs is more challenging. Due to its lower resolution and the fact that Cine MRs are typically 2D rather than 3D volumes. Achieving accurate registration in poorer image quality would represent a significant step toward clinically applicable dose reconstruction. To achieve this goal, one suggestion could be to incorporate the biomechanical properties of components of the insert into the registration methods. This could improve DIR performance, particularly as image quality decreases and go from 3D volumes to 2D images.

In the results for the visualization of the DIR methods, discrepancies between the forward and backward DVFs are revealed when comparing the DVFs obtained with the same DIR method. It would be of interest to further examine the inverse consistency of the three applied DIR methods and look into its impact on the accumulated dose.

A new prototype is currently under development with several adjustments. To minimize the positional uncertainty, the size of the sensitive volume will be increased and will be precisely centered within the envelope. The increasement in size will also enhance dosimetric accuracy. Furthermore, the new prototype will also have fewer loops for the fibers exiting the insert, resulting in less fiber within the radiation field. This adjustment is expected to solve issues related to the reduction of the sensitivity of the PSDs.

V. Conclusion

The novel prototype insert demonstrated its feasibility for validating deformable dose accumulation. Furthermore, all methods used in this study to obtain the accumulated dose were far superior to assuming the planned dose was delivered.

Acknowledgment

The author has supervisors whom acknowledge funding by the Dutch Research Council (NWO) through project no. 18495 (ADEQUATE).

The author also wished to thank the department of radiotherapy at UMC Utrecht, Medscint and IBA QUASAR for their support. Special thanks to the supervisors for always being available to answer all my questions and for the insightful discussions.

References

[1] H Herrmann, Y Seppenwoolde, D Georg, and J Widder. Image guidance: past and future of radiotherapy. *Der Radiologe*, 59(Suppl 1):21, 2019.

[2] Jan JW Lagendijk, Bas W Raaymakers, Cornelis AT Van den Berg, Marinus A Moerland, Marielle E Philippens, and Marco Van Vulpen. Mr guidance in radiotherapy. *Physics in Medicine & Biology*, 59(21):R349, 2014.

[3] Bas W Raaymakers, IM Jürgenliemk-Schulz, GH Bol, M Glitzner, ANTJ Kotte, B Van Asselen, JCJ De Boer, JJ Bluemink, SL Hackett, MA Moerland, et al. First patients treated with a 1.5 t mri-linac: clinical proof of concept of a high-precision, high-field mri guided radiotherapy treatment. *Physics in Medicine & Biology*, 62(23):L41, 2017.

[4] André Buchali, Stefan Koswig, Stefan Dinges, Peter Rosenthal, Jürgen Salk, Gundula Lackner, Dirk Böhmer, Lorenz Schlenger, and Volker Budach. Impact of the filling status of the bladder and rectum on their integral dose distribution and the movement of the uterus in the treatment planning of gynaecological cancer. *Radiotherapy and oncology*, 52(1):29–34, 1999.

[5] Joost J Nuyttens, John M Robertson, Di Yan, and Alvaro Martinez. The variability of the clinical target volume for rectal cancer due to internal organ motion during adjuvant treatment. *International Journal of Radiation Oncology* Biology* Physics*, 53(2):497–503, 2002.

[6] Kimiko Hirata, Michio Yoshimura, Nobutaka Mukumoto, Mitsuhiro Nakamura, Minoru Inoue, Makoto Sasaki, Takahiro Fujimoto, Shinsuke Yano, Manabu Nakata, Takashi Mizowaki, et al. Three-dimensional intrafractional internal target motions in accelerated partial breast irradiation using three-dimensional conformal external beam radiotherapy. *Radiotherapy and Oncology*, 124(1):118–123, 2017.

[7] Dirk Verellen, Mark De Ridder, and Guy Storme. A (short) history of image-guided radiotherapy. *Radiotherapy and Oncology*, 86(1):4–13, 2008.

[8] Brigid A McDonald, Cornel Zachiu, John Christodouleas, Mohamed A Naser, Mark Ruschin, Jan-Jakob Sonke, Daniela Thorwarth, Daniel Létourneau, Neelam Tyagi, Tony Tadic, et al. Dose accumulation for mr-guided adaptive radiotherapy: From practical considerations to state-of-the-art clinical implementation. *Frontiers in oncology*, 12:7471, 2023.

[9] David A Jaffray, Patricia E Lindsay, Kristy K Brock, Joseph O Deasy, and Wolfgang A Tomé. Accurate accumulation of dose for improved understanding of radiation effects in normal tissue. *International Journal of Radiation Oncology* Biology* Physics*, 76(3):S135–S139, 2010.

[10] Alexander JE Raaijmakers, Bas W Raaymakers, and Jan JW Lagendijk. Integrating a mri scanner with a 6 mv radiotherapy accelerator: dose increase at tissue–air interfaces in a lateral magnetic field due to returning electrons. *Physics in Medicine & Biology*, 50(7):1363, 2005.

[11] HM Patrick, Emily Poon, and J Kildea. Experimental validation of a novel method of dose accumulation for the rectum. *Acta Oncologica*, 62(8):915–922, 2023.

[12] Omar Bohoudi, Frank J Lagerwaard, Anna ME Bruynzeel, Nina I Niebuhr, Wibke Johnen, Suresh Senan, Ben J Slotman, Asja Pfaffenberger, and Miguel A Palacios. End-to-end empirical validation of dose accumulation in mri-guided adaptive radiotherapy for prostate cancer using an anthropomorphic deformable pelvis phantom. *Radiotherapy and Oncology*, 141:200–207, 2019.

[13] Uffe Bernchou, Rasmus L Christiansen, Anders Bertelsen, David Tilly, Hans L Riis, Henrik R Jensen, Faisal Mahmood, Christian R Hansen, Vibeke N Hansen, Tine Schytte, et al. End-to-end validation of the geometric dose delivery performance of mr linac adaptive radiotherapy. *Physics in Medicine & Biology*, 66(4):045034, 2021.

[14] Prescilla Uijtewaal, Benjamin Côté, Thomas Foppen, Wilfred de Vries, Simon Woodings, Pim Borman, Simon Lambert-Girard, François Therriault-Proulx, Bas Raaymakers, and Martin Fast. Performance of the hyperscint scintillation dosimetry research platform for the 1.5 t mr-linac. *Physics in Medicine & Biology*, 68(4):04NT01, 2023.

[15] Madelon van den Dobbelsteen, Prescilla Uijtewaal, Sara Hackett, Kalin Penev, Rocco Flores, Stephanie Smith, Yoan LeChasseur, Benjamin Côté, Pim Borman, Bram van Asselen, et al. Best in physics (multi-disciplinary): First experimental demonstration of a deformable phantom insert with integrated plastic scintillation real-time dosimeters on an mr-linac. In *AAPM 65th Annual Meeting & Exhibition*. AAPM, 2023.

[16] David Miller, Kalin Penev, Jennifer Dietrich, Nicholas Hartman, Rocco Flores, and Grant Koenig. Deformable imaging phantom for 4d motion tracking with scintillator radiation detector, 2023. US Patent.

[17] Cornel Zachiu, Nicolas Papadakis, Mario Ries, Chrit Moonen, and B Denis De Senneville. An improved optical flow tracking technique for real-time mr-guided beam therapies in moving organs. *Physics in Medicine & Biology*, 60(23):9003, 2015.

[18] Stefan Klein, Marius Staring, Keelin Murphy, Max A Viergever, and Josien PW Pluim. Elastix: a toolbox for intensity-based medical image registration. *IEEE transactions on medical imaging*, 29(1):196–205, 2009.

[19] B Denis de Senneville, Cornel Zachiu, Mario Ries, and Chrit Moonen. Evolution: an edge-based variational method for non-rigid multi-modal image registration. *Physics in Medicine & Biology*, 61(20):7377, 2016.

[20] Martina Murr, Kristy K Brock, Marco Fusella, Nicholas Hardcastle, Mohammad Hussein, Michael G Jameson, Isak Wahlstedt, Johnson Yuen, Jamie R McClelland, and Eliana Vasquez Osorio. Applicability and usage of dose mapping/accumulation in radiotherapy. *Radiotherapy and Oncology*, 182:109527, 2023.

[21] Haisen S Li, Hualiang Zhong, Jinkoo Kim, Carri Glide-Hurst, Misbah Gulam, Teamour S Nurushev, and Indrin J Chetty. Direct dose mapping versus energy/mass transfer mapping for 4d dose accumulation: fundamental differences and dosimetric consequences. *Physics in Medicine & Biology*, 59(1):173, 2013.

[22] Rojano Kashani, Kwok Lam, Dale Litzenberg, and James Balter. A deformable phantom for dynamic modeling in radiation therapy. *Medical physics*, 34(1):199–201, 2007.

[23] Hendrik Teske, Kathrin Bartelheimer, Jan Meis, Rolf Bendl, Eva M Stoiber, and Kristina Giske. Construction of a biomechanical head and neck motion model as a guide to evaluation of deformable image registration. *Physics in Medicine & Biology*, 62(12):N271, 2017.

[24] Lando S Bosma, Cornel Zachiu, Mario Ries, B Denis de Senneville, and Bas W Raaymakers. Quantitative investigation of dose accumulation errors from intra-fraction motion in mrgrt for prostate cancer. *Physics in Medicine & Biology*, 66(6):065002, 2021.

[25] Un Jin Yeo, JR Supple, ML Taylor, Ryan Smith, Tomas Kron, and RD Franich. Performance of 12 dir algorithms in low-contrast regions for mass and density conserving deformation. *Medical physics*, 40(10):101701, 2013.

[26] Titania Juang, Shiva Das, John Adamovics, Ron Benning, and Mark Oldham. On the need for comprehensive validation of deformable image registration, investigated with a novel 3-dimensional deformable dosimeter. *International Journal of Radiation Oncology* Biology* Physics*, 87(2):414–421, 2013.